Astron. Astrophys. 332, 121–126 (1998)

ASTRONOMY AND ASTROPHYSICS

The Vela X–1 pulse-averaged spectrum as observed by *BeppoSAX*

M. Orlandini[1], D. Dal Fiume[1], F. Frontera[1], G. Cusumano[2], S. Del Sordo[2], S. Giarrusso[2], S. Piraino[2], A. Segreto[2], M. Guainazzi[3], and L. Piro[4]

[1] Istituto Tecnologie e Studio Radiazioni Extraterrestri (TeSRE), C.N.R., Via Gobetti 101, I-40129 Bologna, Italy
[2] Istituto di Fisica Cosmica ed Applicazioni dell'Informatica (IFCAI), C.N.R., Via La Malfa 153, I-90146 Palermo, Italy
[3] *BeppoSAX* Scientific Data Center (SDC), Nuova Telespazio, Via Corcolle 19, I-00131 Roma, Italy
[4] Istituto di Astrofisica Spaziale (IAS), C.N.R., Via Fermi 21, I-00044 Frascati, Italy

Received 18 September 1997 / Accepted 25 November 1997

Abstract. We report on the 20 ksec observation of Vela X–1 performed by *BeppoSAX* on 1996 July 14 during its Science Verification Phase. We observed the source in two intensity states, characterized by a change in luminosity of a factor $\sim$ 2, and a change in absorption of a factor $\sim$ 10. The single Narrow Field Instrument pulse-averaged spectra are well fit by a power law with significantly different indices. This is in agreement with the observed changes of slope in the wide-band spectrum: a first change of slope at $\sim$ 10 keV, and a second one at $\sim$ 35 keV. To mimic this behaviour we used a double power law modified by an exponential cutoff — the so-called NPEX model — to fit the whole 2–100 keV continuum. This functional is able to adequately describe the data, especially the low intensity state. We found an absorption-like feature at $\sim$ 57 keV, very well visible in the ratio performed with the Crab spectrum. We interpreted this feature as a cyclotron resonance, corresponding to a neutron star surface magnetic strength of 4.9×10^{12} Gauss. The *BeppoSAX* data do not require the presence of a cyclotron resonance at $\sim$ 27 keV as found in earlier works.

Key words: binaries: eclipsing – stars: individual: HD 77581 – stars: neutron – pulsars: individual: (Vela X–1) – X-rays: stars

1. Introduction

Among the class of X–ray binary pulsars, Vela X–1 is the one that has been more carefully monitored since its discovery as a pulsator in 1976 (McClintock et al. 1976). It is the prototype of the subclass of pulsars that accrete matter directly from the stellar wind, coming from the massive early-type star HD 77581 (spectral type B0 Ib (Hutchings 1974)). During its orbit around the companion, the X–ray emission from the pulsar suffers substantial photoelectric absorption, increasing until the source is eclipsed by its companion every 8.96 days — the orbital period — for about 1.7 days (Avni 1976). The study of the orbital phase dependence of the low energy absorption due to the circumstellar matter, together with spectroscopic studies of the optical companion, has shown the presence of accretion (Blondin, Stevens & Kallman 1991) and photoionization (Kaper, Hammerschlag-Hensberge & Zuiderwijk 1994) wakes.

The pulse-averaged spectrum of Vela X–1 also shows an Iron emission line centered at $\sim$ 6.4 keV (White, Swank & Holt 1983). Recently, cyclotron resonance features (CRFs) at $\sim$ 27 and 55 keV have been reported by Kretschmar et al. (1996) and Makishima & Mihara (1992).

2. Observation

The *BeppoSAX* satellite is a program of the Italian Space Agency (ASI), with participation of the Netherlands Agency for Aerospace Programs (NIVR), devoted to X–ray astronomical observations in the broad 0.1–300 keV energy band (Boella et al. 1997a). The payload includes four Narrow Field Instruments (NFIs) and two Wide Field Cameras (Jager et al. 1997). The NFIs consist of Concentrators Spectrometers (C/S) with 3 units (MECS) operating in the 1–10 keV energy band (Boella et al. 1997b) and 1 unit (LECS) operating in 0.1–10 keV (Parmar et al. 1997), a High Pressure Gas Scintillation Proportional Counter (HPGSPC) operating in the 3–120 keV energy band (Manzo et al. 1997) and a Phoswich Detection System (PDS) with four scintillation detection units operating in the 15–300 keV energy band (Frontera et al. 1997).

During the Science Verification Phase a series of well known X–ray sources have been observed in order to check the capabilities and performances of the instruments aboard *BeppoSAX*. Vela X–1 is one of these sources and it has been observed by three of the four NFIs (LECS was not operative during this point-

Send offprint requests to: orlandini@tesre.bo.cnr.it

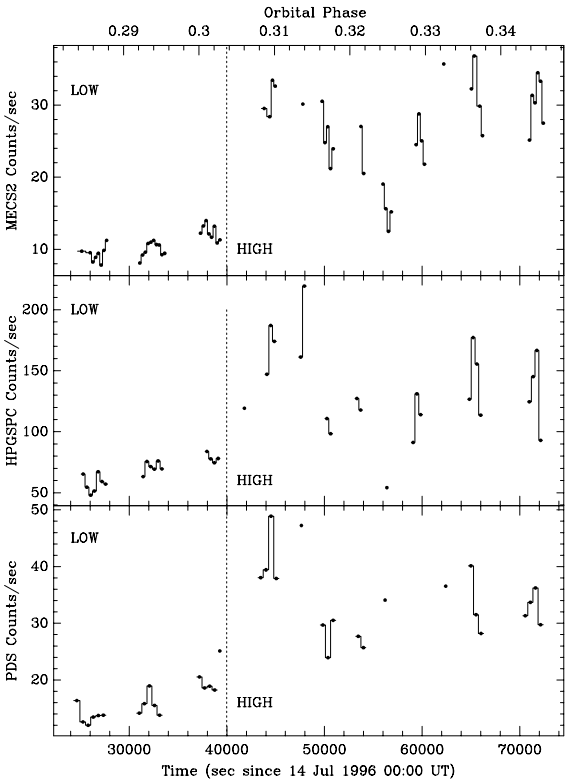

Fig. 1. Vela X-1 background subtracted light curve for all the three operative *BeppoSAX* NFIs instruments. Gaps are due to South Atlantic Anomaly passages and Earth occultations (the average *BeppoSAX* duty cycle is about 50%). The upper scale represents the orbital phase based on the ephemeris given by Deeter et al. (1987). The first panel shows the light curve, rebinned at 283 sec, from one of the three MECS aboard *BeppoSAX*. The second panel shows the 384 sec HPGSPC light curve, while in the third panel the 500 sec PDS data are displayed. In both last cases binning times have been chosen as an integer multiple of the rocking stay time.

ing) on 1996 July 14 from 06:01 to 20:54 UT. The net exposure time for MECS, HPGSPC and PDS was 21.6, 8.1 and 9.5 ksec, respectively. These differences are due to rocking of collimators (see below) and different filtering criteria during passages in the South Atlantic Geomagnetic Anomaly (SAGA) and before and after Earth occultations.

In Fig. 1 we show the average light curve of Vela X–1 as observed by the three operative NFIs instruments. Data were telemetred in direct modes, which provide complete information on time, energy and, if available, position for each photon. The two collimated instruments (HPGSPC and PDS) were operated in rocking mode with a 96 sec stay time for HPGSPC, and 50 sec stay time for PDS, in order to monitor the background along the orbit — a complete on-source observation, apart from SAGA passages and Earth occultations, is possible only for PDS because of its two (mechanical) collimators. The single-collimator HPGSPC will always show stay time gaps in its data.

The first part of the observation (about 40% of the total net time, and marked LOW in the figure) corresponds to one of the common intensity dips showed by Vela X–1, explained as due to passages of the neutron star through clumpy circumstellar material (Sato et al. 1986).

3. Spectral analysis

The pulse-averaged spectrum of Vela X–1 has been fitted separately in the energy bands of the three operative *BeppoSAX* NFIs instruments, and the results are summarized in Table 1. We used XSPEC V9.0 (Arnaud 1996) as spectral fitting program, and we refer to its User Manual[1] for the details of the functionals used for the fits. We treated separately the two intensity states of the source. Note that the high χ^2_ν for PDS spectra is mainly due to systematic uncertainty, below 5% in the fit residuals.

From Table 1 it is evident that any attempt of fitting the wide-band Vela X–1 average spectrum with a single power law, eventually modified by energy cutoff and/or narrow-band absorption features, will be unsuccessful, because of the completely different spectral slopes in the three NFIs energy ranges. Indeed, the usual — for an X–ray pulsar — power law plus high-energy cutoff (White, Swank & Holt 1983) gives a very poor fit to the 2–100 keV spectra, with $\chi^2_\nu \sim 3$ and 9 for the two intensity states (Orlandini et al. 1997a). A fit with a different continuum, namely a power law modified by the so called Fermi–Dirac cutoff (Tanaka 1986), gave an unacceptable fit, too.

Therefore we used for the continuum a spectral law that allowed the flattening of the spectrum observed in the $\sim$ 10–30 keV range. In particular we found that two power laws modified at high energy by the *same* exponential cutoff were able to describe the 2–100 keV spectra, expecially the LOW state. This spectral functional has been chosen as a compromise between a reasonable good fit and a simple law. It is also the same continuum — the so-called NPEX — used by Mihara in fitting the continuum of X–ray pulsars (Mihara 1995).

By including a Gaussian line in emission at $\sim$ 6.4 keV and an absorption edge at $\sim$ 7.7 keV we obtained a reasonable good fit, with χ^2_ν= 1.3 (331 dof) for LOW state, and χ^2_ν= 2.8 (332 dof) for HIGH state. From the form of the residuals at high energy we were led to add CRFs in the spectrum description. Other authors (Makishima & Mihara 1992, Kretschmar et al. 1996) have considered the fundamental cyclotron resonance at $\sim$ 27 keV, but our high energy data from both HPGSPC and PDS do not show it. Therefore we added to our model a CRF at $\sim$ 57. Both a Lorenzian (Mihara 1995) or a Gaussian in absorption (Soong et al. 1990) model gave a quite good fit, especially for the LOW state. The fit results are summarized in Table 2 and the fits for the two intensity states are shown in Fig. 2. The inter-calibration between the NFIs is quite good, expecially at the light of this early calibration status[2]. With MECS2 as reference, normalization is 0.98 for HPGSPC, and 0.79 for PDS.

Our results on the Iron line energy at 6.4 keV are in agreement with those found by other experiments. A more detailed

[1] The XSPEC User Manual is available on-line at http://legacy.gsfc.nasa.gov/docs/xanadu/xspec/u_manual.html

[2] Updated information on the calibration status are available at http://www.sdc.asi.it/software/

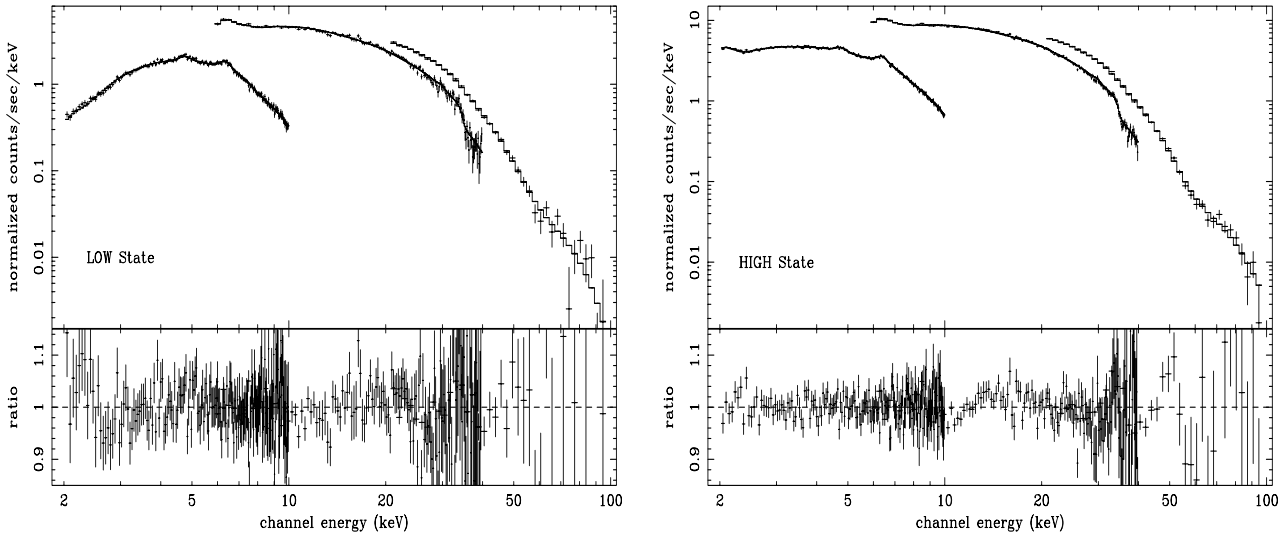

Fig. 2. *BeppoSAX* Vela X–1 pulse-averaged spectra in the two intensity states: LOW on the left and HIGH on the right. The continuum has been modelled by two power laws plus the same exponential cutoff. We added an emission line, an absorption edge and a Lorenzian cyclotron resonance at $\sim$ 57 keV. Note the dramatic change in the low energy absorption.

Table 1. *BeppoSAX* NFIs spectral fits to Vela X–1 pulse-averaged spectrum. MECS data are fit by a single power law, plus photoelectric absorption, an emission Gaussian line and an absorption edge. The HPGSPC spectrum is fit by a power law with exponential cutoff plus an emission Gaussian line (the inclusion of a CRF did not improve the fit). The PDS data have been fit with a power law modified by a high-energy cutoff of the form $\exp[(E_c - E)/E_f]$, plus a Lorenzian CRF.

	MECS (2–10 keV)			**HPGSPC (6–40 keV)**			**PDS (20–100 keV)**		
LOW	N_H	6.5 ± 0.3	(10^{22} cm^{-2})	E_c	$9.6^{+0.5}_{-0.4}$	(keV)	E_c	35 ± 1	(keV)
	α	$0.93^{+0.01}_{-0.06}$		α	-0.32 ± 0.09		α	2.2 ± 0.1	
	E_{Fe}	6.42 ± 0.03	(keV)	E_{Fe}	$6.44^{+0.04}_{-0.05}$	(keV)	E_f	17^{+8}_{-2}	(keV)
	σ_{Fe}	0.10 ± 0.07	(keV)	σ_{Fe}	0.10 (fixed)	(keV)	Depth	$0.9^{+0.01}_{-0.2}$	
	EW	110 ± 25	(eV)	EW	375 ± 130	(eV)	Width	10^{+13}_{-8}	(keV)
	E_{edge}	7.6 ± 0.2	(keV)				E_{cyc}	56 ± 2	(keV)
	τ_{edge}	0.15 ± 0.03							
	Flux[a]	0.24		Flux[a]	0.34		Flux[a]	0.07	
	Luminosity[b]	0.98		Luminosity[b]	3.6		Luminosity[b]	1.4	
	χ^2_ν (dof)	1.048 (163)		χ^2_ν (dof)	1.167 (127)		χ^2_ν (dof)	1.501 (29)	
HIGH	N_H	$0.86^{+0.10}_{-0.07}$	(10^{22} cm^{-2})	E_c	$9.3^{+0.3}_{-0.2}$	(keV)	E_c	39 ± 2	(keV)
	α	0.91 ± 0.03		α	-0.40 ± 0.05		α	$2.1^{+0.2}_{-0.3}$	
	E_{Fe}	6.46 ± 0.02	(keV)	E_{Fe}	$6.40^{+0.04}_{-0.05}$	(keV)	E_f	16 ± 1	(keV)
	σ_{Fe}	0.10 (fixed)	(keV)	σ_{Fe}	0.10 (fixed)	(keV)	Depth	1.2 ± 0.2	
	EW	115 ± 10	(eV)	EW	380 ± 100	(eV)	Width	12 ± 1	(keV)
	E_{edge}	$7.5^{+0.2}_{-0.1}$	(keV)				E_{cyc}	57 ± 1	(keV)
	τ_{edge}	0.09 ± 0.02							
	Flux[a]	0.62		Flux[a]	0.64		Flux[a]	0.14	
	Luminosity[b]	2.2		Luminosity[b]	6.8		Luminosity[b]	2.8	
	χ^2_ν (dof)	1.126 (164)		χ^2_ν (dof)	1.720 (127)		χ^2_ν (dof)	1.969 (29)	

NOTE — All quoted errors represent 90% confidence level for a single parameter.

[a] Total flux in each instrument energy band, in units of photons cm^{-2} sec^{-1}.

[b] Total X–ray luminosity in each instrument energy band, in units of 10^{36} ergs sec^{-1}, assuming a distance of 1.9 kpc (Sadakane et al. 1985).

Table 2. Fit results on the wide-band *BeppoSAX* Vela X–1 pulse-averaged spectra in the two intensity states. Also an absorption Gaussian at 57 ± 1 keV, with width 22 ± 1 keV FWHM, and Equivalent Width 30 ± 3 keV fits well the CRF. All quoted errors represent 90% confidence level for a single parameter.

	LOW State	**HIGH State**
N_H (10^{22} cm^{-2})	$5.6^{+0.3}_{-0.2}$	0.7 ± 0.1
α_1	-2.1 ± 0.5	-1.1 ± 0.2
I_1 [a]	$(5 \pm 2) \times 10^{-4}$	$(4 \pm 3) \times 10^{-3}$
α_2	0.34 ± 0.11	0.26 ± 0.07
I_2 [a]	0.13 ± 0.01	0.34 ± 0.03
E_c (keV)	9.6 ± 1.8	9.2 ± 0.8
E_{Fe} (keV)	6.42 ± 0.04	6.45 ± 0.02
σ_{Fe} (keV)	0.10 (fixed)	0.10 (fixed)
I_{Fe} (Ph cm^{-2} s^{-1})	$(4.2^{+0.9}_{-0.7}) \times 10^{-3}$	$(7.6^{+0.6}_{-0.9}) \times 10^{-3}$
E_{edge} (keV)	$7.7^{+0.2}_{-0.1}$	$7.4^{+0.2}_{-0.1}$
E_{cyc} (keV)	53^{+2}_{-1}	$54.4^{+1.5}_{-0.2}$
Depth	$1.5^{+0.7}_{-0.6}$	$1.3^{+0.4}_{-0.1}$
Width (keV)	20^{+4}_{-7}	17^{+3}_{-2}
χ^2_ν (dof)	1.198 (330)	1.797 (330)

[a] Photons cm^{-2} sec^{-1} keV^{-1} at 1 keV.

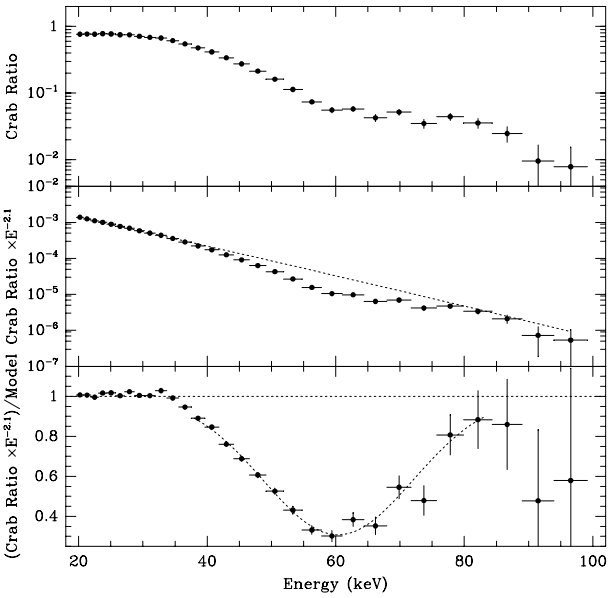

Fig. 3. *Upper panel*: Ratio between the PDS Vela X–1 and Crab spectra. Note the change of slope at $\sim$ 57 keV. *Middle panel*: the Vela X–1/Crab ratio multiplied by $E^{-2.1}$, the functional form of the Crab spectrum. Deviations from the continuum (dotted line) occur for $E \gtrsim 35$ keV. *Lower panel*: ratio between the (Vela X–1/Crab ratio $\times$ $E^{-2.1}$) and the functional form of the Vela X–1 continuum as derived from the wide-band fit. A Gaussian fit to the CRF (dotted line) is also shown.

discussion on the properties of the Iron line, with emphasis on its pulse-phase variation, will be discussed in a separate paper.

4. Discussion

4.1. The X–ray continuum

This is the first time that we have three (quite different) X–ray detectors that *simultaneously* observed Vela X–1 in a so wide energy range. From the single NFIs spectra we can extrapolate that the wide-band spectrum will have a complex form: up to $\sim$ 10 keV it is very well described by a simple power law (MECS data). Then the spectrum begins to flatten: first at $\sim$ 10 keV (cutoff in HPGSPC data) and then more pronouncedly after $\sim$ 35 keV (cutoff in PDS data). These variations are quite in agreement with the change observed in the Vela X–1 pulse profile, from a five-peaked to a two-peaked shape just in the 10–30 keV range (see e.g., Orlandini 1993).

The NPEX functional that we used in the wide-band spectral fitting is surely a crude approximation of this behaviour, but it describes the data very well for the LOW state, and reasonably well for the HIGH state. It is important to stress how the choice of the functional describing the continuum has dramatic effects on the line characteristics. Indeed, a fit to our data with a power law modified by a high energy cutoff of the type described by White, Swank & Holt (1983) was not able to well describe both the $\sim$ 27 and $\sim$ 57 keV CRFs (Orlandini et al. 1997a).

4.2. Cyclotron resonance features

The Vela X–1 pulse-averaged spectrum shows all the features present in a typical X–ray binary pulsar spectrum, namely an Iron emission line with its absorption edge, and signatures of cyclotron resonance. While the Iron line feature is clearly determined in the spectrum, there are ambiguities in the position of the fundamental CRF. Indeed, a fit to the wide-band *BeppoSAX* spectrum with an NPEX and two CRFs, with the fundamental constrained in the 10–40 keV range, produced a cyclotron energy at $\sim$ 24 keV and a χ^2_ν comparable with those shown in Table 2, although the CRF depth was extremely low. An F–test was not successful in discriminating between the two hypotheses, with a probability of chance improvement of 98% for LOW State and 42% for HIGH State.

But there are some arguments against the low energy CRF: first, the HPGSPC would surely be successful in its detection if it had the same characteristics as in Mihara (1995), while the inclusion of such feature did not improve the fit. Second, a pulse-phase spectroscopy on the PDS data alone shows again that a $\sim$ 27 keV CRF is not detected, but only the $\sim$ 57 keV CRF fits well the data (Orlandini et al. 1997b). Also a ratio between PDS spectra taken during the pulse peaks and those taken during the valleys did not show any variation at $\sim$ 27 keV, but only at $\sim$ 57 keV.

But the most striking result has been obtained by performing the ratio between the PDS Vela X–1 and Crab count rate spectra. This ratio has the advantage of minimizing the effects due to the

Table 3. Fit results on the Vela X–1 CRF. Errors represent 90% confidence level.

	Gaussian	**Lorenzian**
$E_{\rm cyc}$ (keV)	60.4 ± 0.7	59.2 ± 0.6
$\sigma_{\rm cyc}$ (keV)	11.6 ± 0.5	22 ± 1
χ^2_ν (dof)	1.275 (12)	6.662 (12)

detector response and uncertainties in the calibrations. As we can see from the upper panel in Fig. 3, there is an evident change of slope at $\sim$ 57 keV. The same ratio performed on the Hercules X–1 spectrum shows a change of slope at $\sim$ 40 keV, just its well known cyclotron energy (Dal Fiume et al. 1997).

To better enhance the effect due to CRFs, we multiplied the Vela X–1/Crab Ratio by the functional form of the Crab spectrum, *i.e.* a simple power law with index equal to 2.1. In this way we point out deviations of the Vela X–1 spectrum from its continuum without making any assumption on its form. The result is shown in the second panel of Fig. 3, where it is evident that deviations occur only at E $\gtrsim$ 35 keV.

Finally, in the lower panel we show the ratio between the previous function and the Vela X–1 continuum functional, with α_1, α_2, and E_c taken from Table 2. In this way we enlarge all the effects due to line features, although we introduce a model dependence. We can clearly see the absorption feature at $\sim$ 60 keV, that we fit between 40 and 80 keV with both a Gaussian (shown in the figure) and a Lorenzian. The results are shown in Table 3 and seem to indicate a preference for the Gaussian shape.

Because of these considerations we will interpret the $\sim$ 57 keV CRF as the fundamental cyclotron resonance. This corresponds to a surface magnetic field strength of 4.9×10^{12} Gauss, in agreement with theoretical considerations about a high magnetic field in Vela X–1 (Börner et al. 1987).

At the cyclotron resonance frequency ω_c, electrons at rest absorb photons of energy $\hbar\omega_c$. For moving, thermal electrons the Doppler broadening $\Delta\omega_D$ is predicted to be (Mèszàros 1992)

$$\Delta\omega_D = \omega_c \left(\frac{2kT_e}{m_e c^2}\right)^{1/2} |\cos\theta| \qquad (1)$$

where kT_e is the electron temperature, and $m_e c^2$ is the electron rest mass. The angle θ measures the direction of the magnetic field with respect to the line of sight. Outside the range $\omega_c \pm \Delta\omega_D$ the cyclotron absorption coefficient decays exponentially, and other radiative processes become important. From Eq. 1 and the CRF parameters given in Table 2 we obtain a lower limit to the electron temperature of $\sim$ 8 keV, in fair agreement with the calculations of self-emitting atmospheres of Harding et al. (1984). A $\sim$ 27 keV CRF would corresponds to an electron temperature, assuming the same FWHM, of $\sim$ 34 keV: a bit too high. On the other hand, by imposing $kT_e \sim 8$ keV would correspond to a CRF FWHM of $\sim$ 10 keV that should be clearly visible in our spectra.

Finally, the $\sim$ 57 keV CRF agrees with the empirical positive correlation found between the magnetic field strength and the spectral hardness, whether defined in terms of hardness ratio (Frontera & Dal Fiume 1989) or high energy cutoff (Makishima et al. 1990).

5. Conclusions

The wide-band average spectrum of Vela X–1 as observed by *BeppoSAX* appears to be quite complex, showing a progressive change of slope: first at $\sim$ 10 keV and then at $\sim$ 35 keV, just in the same interval where the Vela X–1 pulse profile changes from a five-peak to a two-peak shape. This is clearly visible in the single NFIs spectra, described by power laws with significantly different indices. We approximate this behaviour with a double power law modified by an exponential cutoff (the so called NPEX model). From the form of the residuals we added a cyclotron resonance in the fitting functional: the *BeppoSAX* data do not require a CRF at $\sim$ 27, as found in earlier works, but only at $\sim$ 57 keV. A possible explanation could be an intrinsic variability in the cyclotron resonance, or an effect due to the change of slope of the continuum, not previously taken into account. A better description of the continuum, beyond the scope of this paper is surely needed.

Acknowledgements. The authors wish to thank the *BeppoSAX* Scientific Data Center staff for their support during the observation and data analysis. This research has been funded in part by the Italian Space Agency.

References

Arnaud, K.A. 1996, in Proceedings of V ADASS Symposium, eds. Jacoby, G.H. and Barnes, J., ASP Conf. Series 101, p.17
Avni, Y. 1976, ApJ, 209, 574
Blondin, J., Stevens, I., Kallman, T.R. 1991, ApJ, 371, 684
Boella, G., Butler, R.C., Perola, G.C., Piro, L., Scarsi, L., Bleeker, J. 1997a, A&AS, 122, 299
Boella, G., Chiappetti, L., Conti, G. et al. 1997b, A&AS, 122, 327
Börner, G., Hayakawa, S., Nagase, F., Anzer, U. 1987, A&A, 182, 63
Dal Fiume, D., Orlandini, M., Frontera, F. et al. 1997, A&A, accepted
Deeter, J.E., Boynton, P.E., Shibazaki, N., Hayakawa, S., Nagase, F., Sato, N. 1987, AJ, 93, 877
Frontera, F., Dal Fiume, D. 1989, in Proceedings 23$^{\rm th}$ ESLAB Symposium, ESA Publ. Div. SP–296, p.57
Frontera, F., Costa, E., Dal Fiume, D., Feroci, M., Nicastro, L., Orlandini, M., Zavattini, G. 1997, A&AS, 122, 357
Harding, A.K., Mèszàros, P., Kirk, J.K., Galloway, D.J. 1984, ApJ, 278, 369
Hutchings, J.B. 1974, ApJ, 192, 685
Jager, R., Mels, W.A., Brinkman, A.C. et al. 1997, A&AS, in press
Kaper, L., Hammerschlag-Hensberge, G., Zuiderwijk, E. 1994, A&A, 289, 846
Kretschmar, P., Pan, H.C., Kendziorra, E. et al. 1996, A&AS, 120C, 175

Makishima, K., Mihara, T. 1992, in Frontiers of X–ray Astronomy, eds. Tanaka, Y. and Koyama, K., Universal Academy Press, Tokyo, p.23
Makishima, K., Mihara, T., Ohashi, T. et al. 1990, ApJ, 365, L59
Manzo, G., Giarrusso, S., Santangelo, A., Ciralli, F., Fazio, G., Piraino, S., Segreto, A. 1997, A&AS, 122, 341
McClintock, J.E., Rappaport, S., Joss, P.C. et al. 1976, ApJ, 206, L99
Mèszàros, P. 1992, High-energy Radiation from Magnetized Neutron Stars, University of Chicago Press, p.123
Mihara, T. 1995, PhD thesis, Institute of Physical and Chemical Research, Cosmic Radiation Laboratory
Orlandini, M. 1993, MNRAS, 264, 181
Orlandini, M., Dal Fiume, D., Nicastro, L. et al. 1997a, in Fourth Compton Symposium, a Conference Proceeding, eds. Dermer, C.D. and Kurfess, J.D. American Institute of Physics Press, in press
Orlandini, M., Dal Fiume, D., Nicastro, L., Palazzi, E., Frontera, F. 1997b, in The Cosmic Physics of 2000, ed. Treves, A., SIF Conference Proceedings, Bologna, in press
Parmar, A.N., Martin, D.D.E., Bavdaz, M. et al. 1997, A&AS, 122, 309
Sadakane, K., Hirata, R., Jugako, J., Kondo, Y., Matsuoka, M., Tanaka, Y. 1985, ApJ, 288, 284
Sato, N., Hayakawa, S., Nagase, F., Masai, K., Dotani, T., Inohue, H., Makino, F. 1986, PASJ, 38, 731
Soong, Y., Gruber, D.E., Peterson, L.E., Rothschild, R.E. 1990, ApJ, 348, 641
Tanaka, Y. 1986, in Radiation Hydrodynamics in Stars and Compact Objects, eds. Mihalas, D. and Winkler, K.H., Springer, Berlin, p.198
White, N.E., Swank, J.H., Holt, S.S. 1983, ApJ, 270, 711

This article was processed by the author using Springer-Verlag LaTeX A&A style file *L-AA* version 3.